The Role of Frozen Spins in the Exchange Anisotropy of Core–Shell Fe@Fe_3O_4 Nanoparticles: Supporting Information

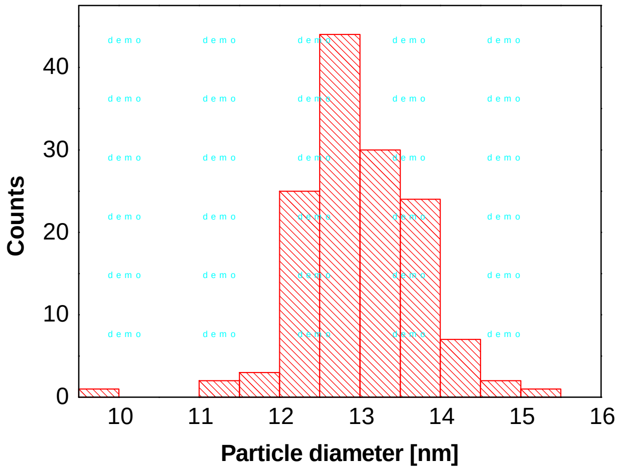

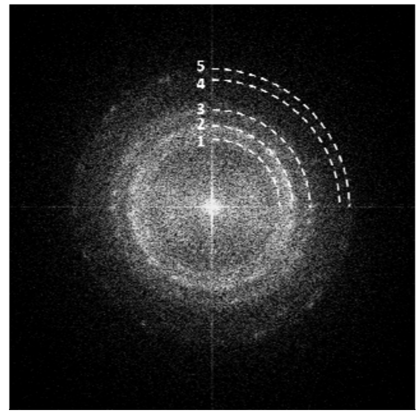

Ring #	Measured *d*-spacing (nm)	*d*-spacing (nm) JCPDS# 79-0418	*(hkl)*
1	0.30	0.2969	220
2	0.26	0.2532	311
3	0.21	0.2099	400
4	0.16	0.1616	333
5	0.15	0.1484	440

Figure S1. (Left) Statistical analysis of particle size (13.0 ± 0.7 nm, *N*=XXX). (Right and bottom) electron diffraction analysis of Fe@Fe_3O_4 core-shell nanoparticles, derived by FFT of the HRTEM image in Figure 1 (inset).

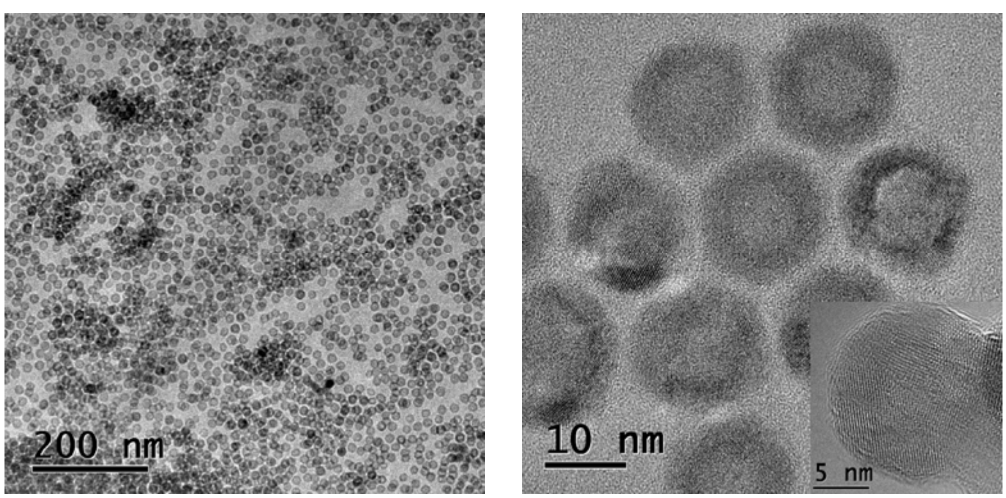

Figure S2. (Left) TEM image (Titan F-30, 300 kV) showing monodispersity of Fe_3O_4 hollow nanoparticles. (Right) HRTEM images (Titan F-30, 300 kV) of the hollow nanoparticles.

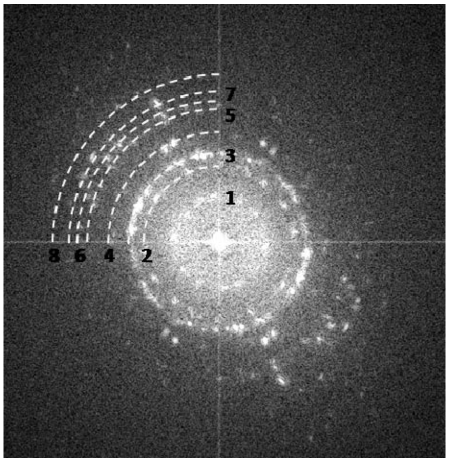

Ring #	Measured d-spacing (nm)	d-spacing (nm) JCPDS 79-0418	(hkl)
1	0.49	0.4848	111
2	0.29	0.2969	220
3	0.25	0.2532	311
4	0.21	0.2099	400
5	0.17	0.1714	422
6	0.16	0.1616	333
7	0.15	0.1484	440
8	0.13	0.1327	620

Figure S3. Electron diffraction analysis of hollow Fe_3O_4 nanoparticles, using the FFT of a HRTEM image (Figure S2, inset).

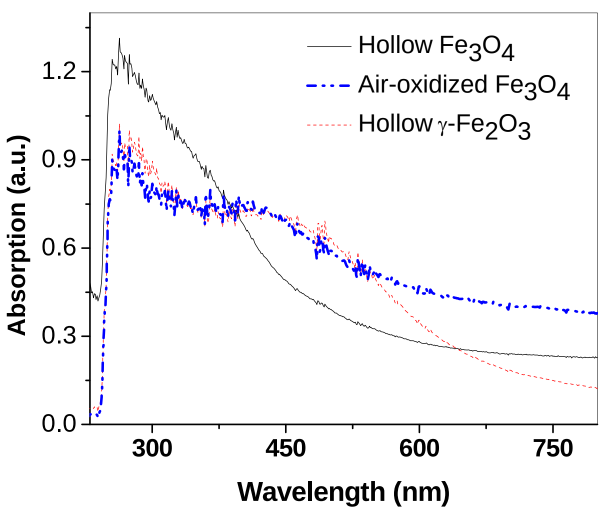

Figure S4. Optical absorption spectra of freshly prepared hollow Fe_3O_4 nanoparticles, by oxidation with $(CH_3)_3NO$ (—), (ii) hollow iron-oxide nanoparticles prepared by oxidation in air (···), and hollow γ-Fe_2O_3 nanoparticles prepared according to Ref. 16 (---).

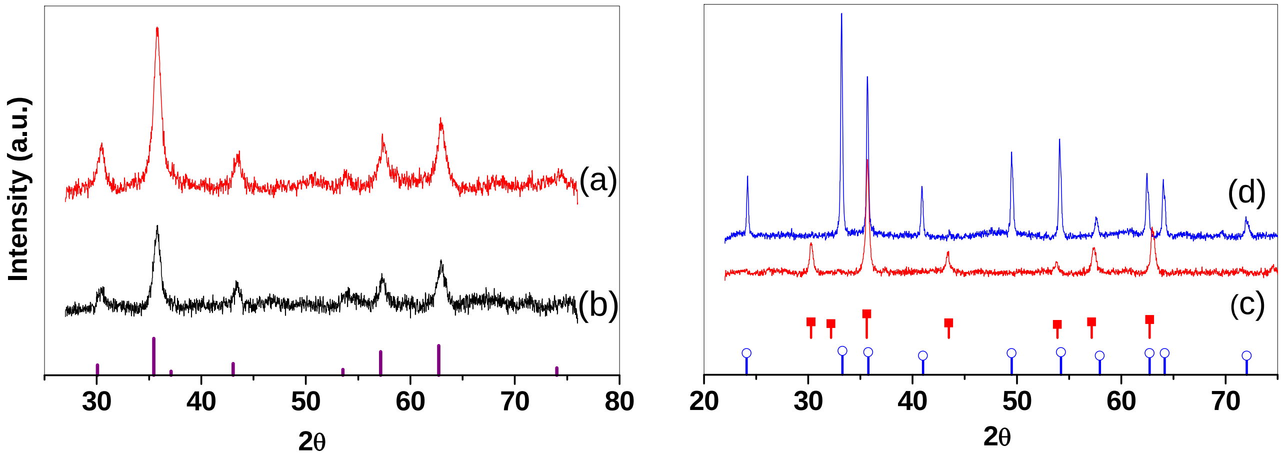

Figure S5. (Left) X-ray diffraction spectra of hollow Fe_3O_4 nanoparticles, before (a) and after (b) heating at 500 °C. (Right) (c) X-ray diffraction spectra of γ-Fe_2O_3 nanoparticles; (d) hollow iron-oxide nanoparticles with conversion to α-Fe_2O_3, after heating at 500 °C.

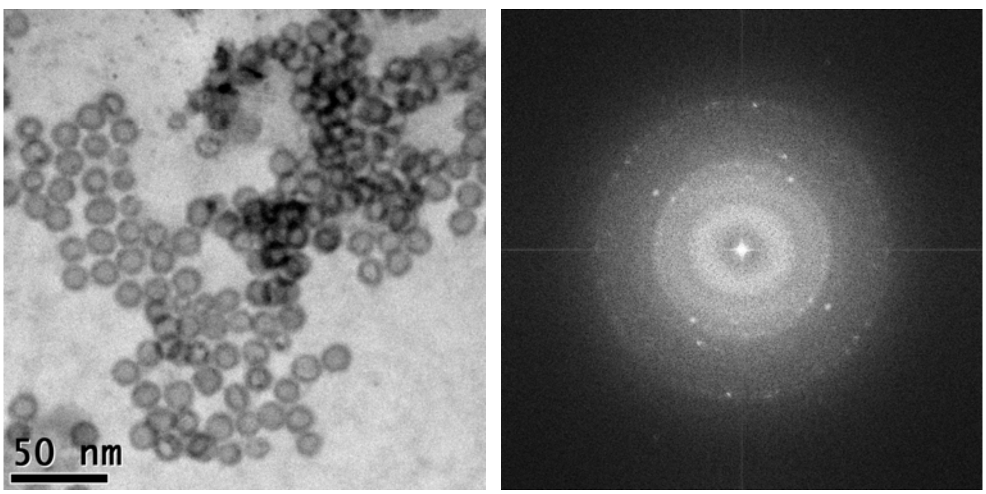

Figure S6. TEM image (Titan F-30, 300 kV) and corresponding FFT of aged nanoparticles after annealing at 400 °C in argon, indicating a solid-to-hollow transition.